

## Size dependent fluorescence spectroscopy of nanocolloids of ZnO

Litty Irimpan,<sup>a)</sup> V. P. N. Nampoory, and P. Radhakrishnan

*International School of Photonics, Cochin University of Science and Technology, Cochin, Kerala, India*

A. Deepthy

*Amrita Institute of Medical Sciences, Cochin, India*

Bindu Krishnan

*Centre for Materials for Electronics Technology, Thrissur, India*

(Received 30 March 2007; accepted 23 July 2007; published online 27 September 2007)

In this article we present size dependent spectroscopic observations of nanocolloids of ZnO. ZnO is reported to show two emission bands, an ultraviolet (UV) emission band and another in the green region. Apart from the known *band gap* 380 nm and *impurity* 530 nm emissions, we have found some peculiar features in the fluorescence spectra that are consistent with the nanoparticle size distribution. Results show that additional emissions at 420 and 490 nm are developed with particle size. The origin of the visible band emission is discussed. The mechanism of the luminescence suggests that UV luminescence of ZnO colloid is related to the transition from conduction band edge to valence band, and visible luminescence is caused by the transition from deep donor level to valence band due to oxygen vacancies and by the transition from conduction band to deep acceptor level due to impurities and defect states. A correlation analysis between the particle size and spectroscopic observations is also discussed. © 2007 American Institute of Physics.

[DOI: [10.1063/1.2778637](https://doi.org/10.1063/1.2778637)]

### I. INTRODUCTION

Semiconductor nanoparticles have been under continuous scientific interest because of their unique quantum nature, which changes the material solid-state properties.<sup>1</sup> ZnO is a wide and direct band gap (approximately 3.37 eV) II–VI semiconductor with many applications, such as a transparent conductive contact, thin-film gas sensor, varistor, solar cell, luminescent material, surface electroacoustic wave device, heterojunction laser diode, ultraviolet (UV) laser, and others.<sup>2</sup> Recently, the interest of the short wavelength display device is increasing. Although laser diode or light emitting diode using GaN was already reported, ZnO has several fundamental advantages over its chief competitor, GaN: (1) its free exciton is bound with 60 meV, much higher than that of GaN (21–25 meV); (2) it has a native substrate; (3) wet chemical processing is possible; and (4) it is more resistant to radiation damage.<sup>3</sup> Optical UV lasing, at both low and high temperatures, has already been demonstrated, although efficient electrical lasing must await the additional development of good *p*-type material.<sup>4</sup> The growth mechanisms and potential applications of these nanostructures have been reviewed by Wang.<sup>5</sup>

The possibility of tailor making of bulk material properties by varying the size, structure, and composition of constituting nanoscale particles makes them candidates for various important applications in the field of material research. Optical methods give rich experimental information about an energetic structure of these finite-size solids. Understanding of size-dependent optical properties of semiconductor clusters has been achieved in a number of theoretical publica-

tions for a long time.<sup>6</sup> Development of methods of preparation and stabilization of monodispersed semiconductor nanoparticles in transparent colloids offer a good opportunity of experimental verification of theoretical predictions.

The ZnO bulk or nanoparticles have various luminescence transitions as different preparation techniques lead to varying structures and surface properties in ZnO. Generally, ZnO exhibits two kinds of emissions: one is at ultraviolet near band-edge emission at approximately 380 nm and the other a visible deep level emission with a peak in the range from 450 to 730 nm.<sup>7</sup> Out of the different reported emission peaks, the origin of the green emission is the most controversial.

Stoichiometric zinc oxide is an insulator that crystallizes with the wurtzite structure to form transparent needle-shaped crystals. The structure contains large voids which can easily accommodate interstitial atoms. Consequently, it is virtually impossible to prepare really pure crystals; also, when these crystals are heated, they tend to lose oxygen.<sup>8</sup> For these reasons, the ZnO shows *n*-type semiconducting properties with many defects, such as lack of oxygen and the excess of zinc. It is known that visible luminescence is mainly due to defects that are related to deep level emissions, such as Zn interstitials and oxygen vacancies. Vanheusden *et al.*<sup>9</sup> found that oxygen vacancies are responsible for the green luminescence in ZnO. Oxygen vacancies occur in three different charge states: the neutral oxygen vacancy ( $V_O^0$ ), the singly ionized oxygen vacancy ( $V_O^*$ ), and the doubly ionized oxygen vacancy ( $V_O^{**}$ ) and only  $V_O^*$  can act as the so-called luminescent centers.<sup>10</sup>

In this article we present size dependent fluorescence emission of colloidal solution of ZnO nanoparticles. ZnO solid has a band gap energy of 3.37 eV and therefore can be

<sup>a)</sup>Electronic mail: [littyirimpan@yahoo.co.in](mailto:littyirimpan@yahoo.co.in)

analyzed by spectroscopic methods in most of the solvents (like diethylene glycol, methanol, propan-2-ol, water) that are transparent in the whole UV–visible spectral regions. Systematic studies by different groups on nanocrystallites have indicated the presence of luminescence due to excitonic emissions as well as significant contribution from surface states on the lower energy side of the photoluminescence (PL) spectrum.<sup>11</sup> It has also been observed that there is difference in the spectra of ZnO of same size prepared by different methods. The effect of method of preparation and surface passivation itself is an indication that the green emission is due to surface states.<sup>12</sup> We have found some peculiarities of the fluorescence spectra that are consistent with the nanoparticle size distribution.

## II. EXPERIMENT

Colloids of ZnO are synthesized by a modified polyol precipitation method.<sup>13,14</sup> The monodisperse ZnO colloidal spheres are produced by a two-stage reaction process. The method of preparation involves the hydrolysis of zinc acetate dihydrate (ZnAc; Merck) in diethylene glycol medium (DEG; Merck). Among the different polyols, diethylene glycol (DEG) is chosen because it is reported to give powders with uniform shape and size distribution. The size of the particles and hence the stability of this colloidal suspension depend on the concentration of zinc acetate as well as on the rate of heating. The molar concentration of precursor solution is varied from 0.01 mM to 0.1 M and when a heating rate of 4 °C/min is employed, ZnO is formed at a temperature of 120 °C. The product from the primary reaction is placed in a centrifuge and the supernatant (DEG, dissolved reaction products, and unreacted ZnAc and water) is decanted off and saved. A secondary reaction is then performed to produce the monodisperse ZnO spheres. Prior to reaching the working temperature, typically at 115 °C, some volume of the primary reaction supernatant is added to the solution. After reaching 120 °C, it is stirred for 1 h to get a monodisperse stable colloid. The ZnO colloids are characterized by optical absorption measurements recorded using a spectrophotometer (JascoV-570 UV/VIS/IR). The cluster sizes are calculated from the absorption spectra using the analytical formula given by Viswanatha *et al.*<sup>15</sup> The structural properties of the sample are investigated by x-ray diffraction (XRD) with Ni-filtered Cu  $K\alpha$  (1.5406 Å) source. The fluorescence emission from ZnO colloids is recorded using a Cary Eclipse fluorescence spectrophotometer (VARIAN).

## III. RESULTS AND DISCUSSIONS

Figure 1 gives the room temperature absorption spectra of the ZnO colloids. The excitonic peak is found to be blue-shifted with decrease in particle size (370–350 nm) with respect to that of bulk ZnO (395 nm) and this could be attributed to the confinement effects.<sup>16</sup> The pronounced dependence of the absorption band gap on the size of ZnO nanocrystals is used to determine the particle size. To get a precise measure of the shift, the first derivative curve of the

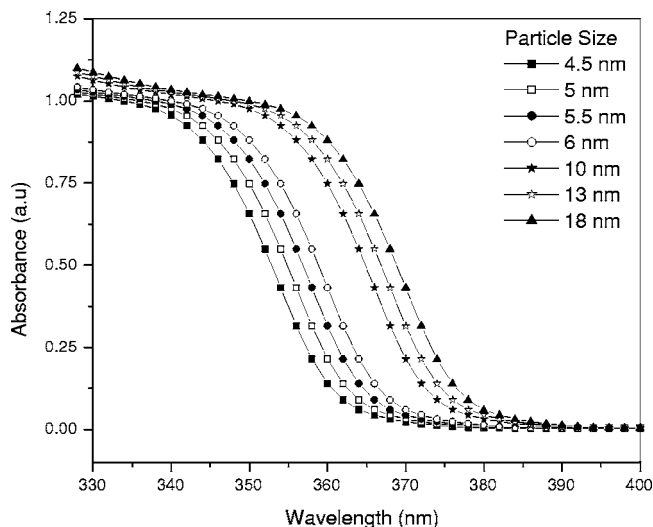


FIG. 1. Optical absorption spectra for colloidal suspensions showing the redshift associated with increased particle size.

absorption spectrum is taken and the point of inflection is taken as the absorption edge. From the shift of absorption edge, the size of the dots is calculated.<sup>15</sup>

The direct band gap of ZnO colloids are estimated from the graph of  $h\nu$  vs  $(\alpha h\nu)^2$  for the absorption coefficient  $\alpha$  that is related to the band gap  $E_g$  as  $(\alpha h\nu)^2 = k(h\nu - E_g)$ , where  $h\nu$  is the incident light energy and  $k$  is the constant. Extrapolation of the linear part until it intersects the  $h\nu$  axis gives  $E_g$ . The optical band gap ( $E_g$ ) is found to be size dependent and there is an increase in the band gap of the semiconductor with a decrease in the particle size as shown in Fig. 2. The total change in the band gap of the material is simultaneously contributed by shifts of the valence and the conduction band edges away from each other. In general, the shift of the top of the valence band (TVB) is not the same as that of the bottom of the conduction band (BCB). Moreover, there are recent studies, though few in number,<sup>17</sup> that report the individual shifts in TVB and BCB as a function of the size employing various forms of high-energy spectroscopies, such as the photoemission and the x-ray absorption spec-

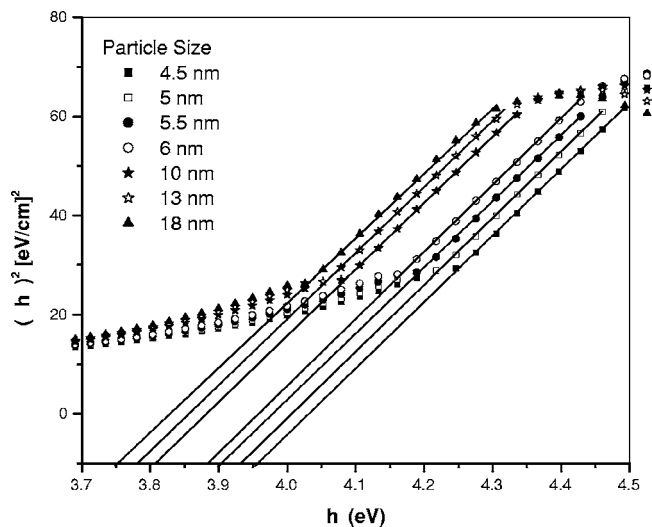


FIG. 2. Optical band gap of ZnO colloids.

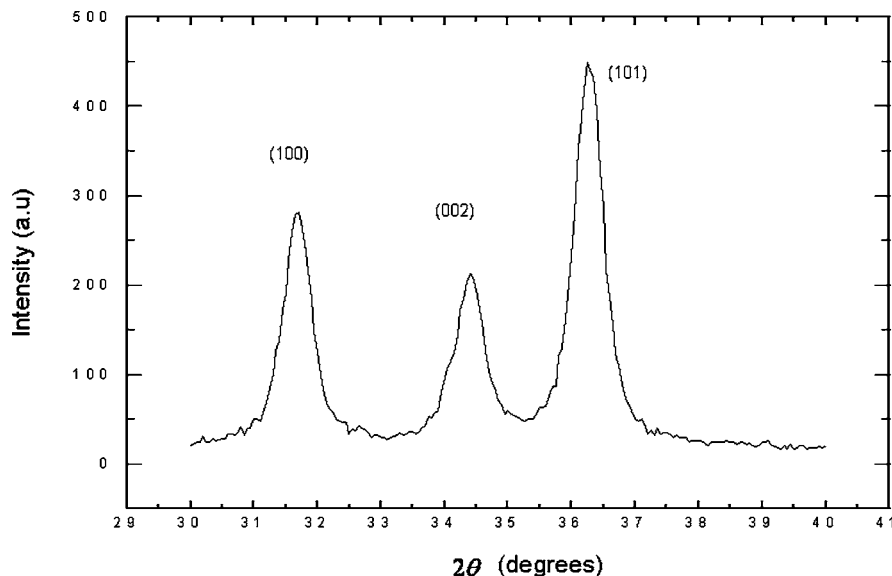


FIG. 3. XRD pattern of the powder extracted from ZnO colloid of size 18 nm.

troscopies. Thus, it is desirable to compute these shifts of the individual band edges with the size of the nanocrystallite. The shifts of the band edges decrease smoothly to zero for large sized nanocrystals in every case and the shift in the BCB is generally much larger compared to the shift in the TVB for any given size of the nanocrystal. This indicates that the shifts in the total band gap as a function of the nanocrystal size are always dominated by the shifts of the conduction band edge in these systems. A larger shift for the BCB is indeed expected in view of the fact that the band-edge shifts are related inversely to the corresponding effective masses<sup>6</sup> and the effective mass of the electron is always much smaller than that of the hole in these II–VI semiconductors. From the band-edge shifts, the electronic structure as a function of the nanocrystallite size can be calculated for semiconductors.<sup>18</sup> The band gap is found to be in the range 3.5–4 eV for the range of particles from 4.5 to 18 nm in agreement with the reported value.<sup>19</sup>

The powder extracted from the colloid of large particle size is characterized by x-ray diffraction. Typical XRD pattern of ZnO colloid is given in Fig. 3. The diffraction pattern and interplane spacings can be well matched to the standard diffraction pattern of wurtzite ZnO, demonstrating the formation of wurtzite ZnO nanocrystals.<sup>20</sup> The particle diameter  $d$  is calculated using the Debye–Scherer formula  $d = 0.89\lambda/(\beta \cos \theta)$  where  $\lambda$  is the x-ray wavelength (1.5406 Å),  $\theta$  is the Bragg diffraction angle, and  $\beta$  is the peak width at half maximum.<sup>21</sup> The XRD peak at 36° in Fig. 3 gives the ZnO particle diameter of 18 nm and matches well with the size calculated from absorption spectrum.

Figure 4 shows the excitation spectrum for an emission peak of 390 nm and peaks at 255 and 325 nm. As ZnO has a broadband absorption, excitation spectrum is very significant in finding the excitation wavelengths at which it has maximum emission. The fluorescence spectra of nano-ZnO colloids of different particle size for an excitation wavelength of 255 nm are shown in Fig. 5. Results show that additional emissions at 420 and 490 nm are developed with increase in particle size along with the known *band gap* 380 nm and *impurity* 530 nm emissions. Figure 6 shows the fluorescence

spectrum of the powder extracted from ZnO colloid of 18 nm at an excitation wavelength of 255 nm. It exhibits all the characteristic emission peaks of the colloid. It confirms the fact that the emission peaks are of pure ZnO and there are no solvent effects.

The UV emission band is assigned to a direct *band gap* transition. Like the absorption spectrum, this UV band undergoes a redshift with particle size. Such size dependent optical properties of semiconductor particle suspensions in the quantum regime are well known and similar observations have previously been made for several quantum particle systems.<sup>6</sup> For the intrinsic luminescence of ZnO nanoparticles, it is generally known that the formation of nanoparticles causes a redshift in the PL spectra due to quantum size effect.<sup>22</sup> An analytical approximation for the lowest eigenvalue (i.e., the first excited electronic state) is described as follows:<sup>6</sup>

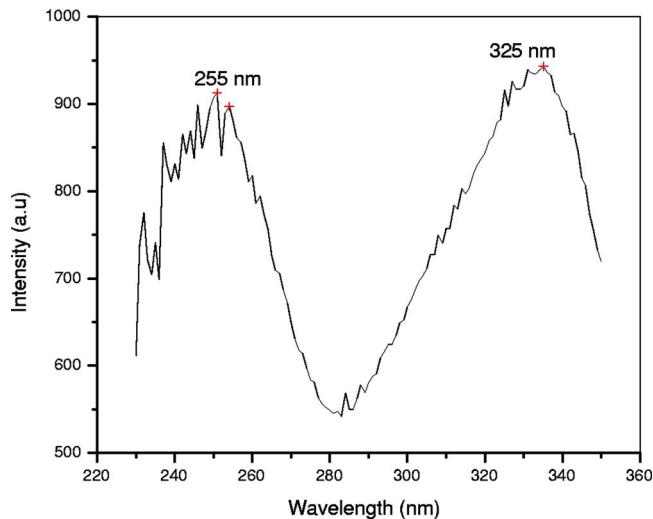


FIG. 4. Excitation spectrum of ZnO colloid for an emission peak of 390 nm.

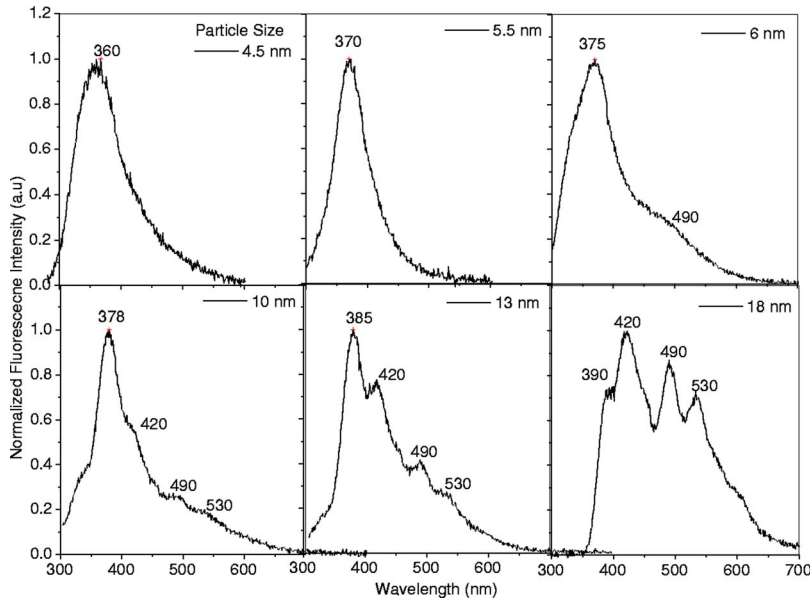


FIG. 5. Steady state fluorescence spectra of nano-ZnO colloids of different particle size for an excitation wavelength of 255 nm.

$$E^* = E_g + \frac{h^2}{8R^2} \left( \frac{1}{m_e} + \frac{1}{m_h} \right) - \frac{1.8e^2}{\epsilon R} + \text{smaller terms,}$$

where  $E_g$  is the band gap, 3.377 eV, for bulk ZnO,<sup>22</sup>  $R$  is the radius of the ZnO nanoparticles,  $h$  is Planck's constant,  $m_e=0.24m_0$  is the electron effective masses,  $m_h=0.45m_0$  is the hole effective masses, and  $\epsilon$  is the dielectric constant of ZnO with an accepted value of 3.7. Results show that the fluorescence emission peak shifts from 360 to 370 nm as the particle size increases from 4.5 to 6 nm as is evident from the previous equation. The emission around 360 nm (3.4 eV) shown in Fig. 5 is consistent with band gap of the ZnO nanoparticles. A redshift of UV emission is observed with the increase in the particle size which accords quantum size effects.

With the increase in the particle size, the energy of UV luminescence is shifted from 3.5 eV (350 nm) to 3 eV (390 nm). The shift of band gap energy is related to the structural property. Therefore, the energy of UV emission known as

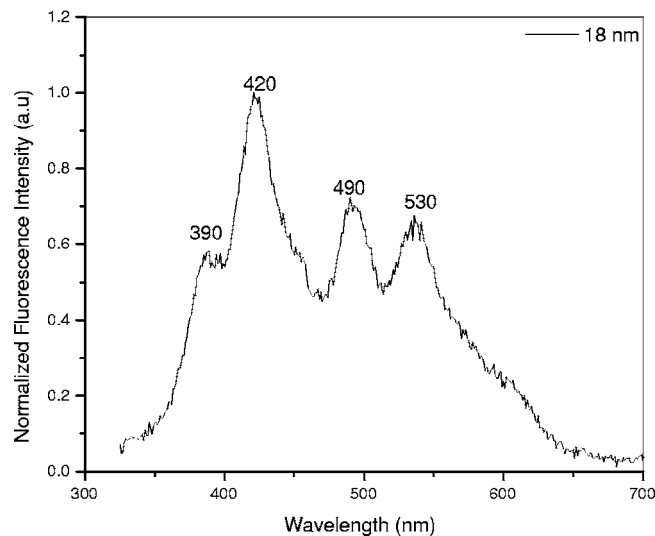


FIG. 6. Fluorescence spectrum of the powder extracted from ZnO colloid of size 18 nm at an excitation wavelength of 255 nm.

near band-edge emission is decreased from 3.5 to 3 eV. The band gap is found to be in the range 3.5–4 eV for the range of particles from 4.5 to 18 nm as shown in Fig. 2. The optical band gap is shifted from 3.5 to 4 eV for different particle size and the shift is consistent with the result of PL in the range of UV. The UV emission is shifted from 3.5 to 3 eV by the shift of optical band gap from 4 to 3.5 eV and it clearly indicates that the origin of UV emission is the near band-edge emission.

Mean cluster size could be principally derived from the absorption onset measurements and the enlargement effects are expected to be predominant when the particle size is less than about 6 nm as shown in Fig. 7(a) where the band enlargement is plotted as a function of the average particle size. Figure 7(b) shows the energy of the band to band transition as a function of the mean particle size. The redshift in the

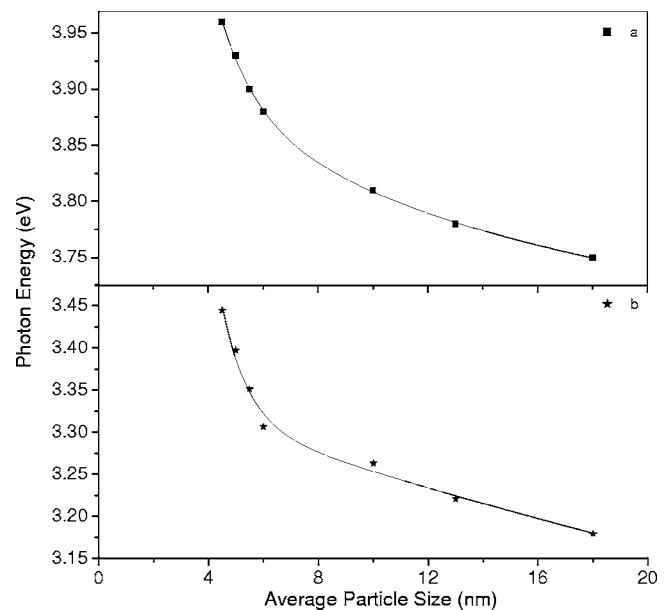


FIG. 7. Dependence of mean particle size on (a) band gap enlargement and (b) band to band emission.



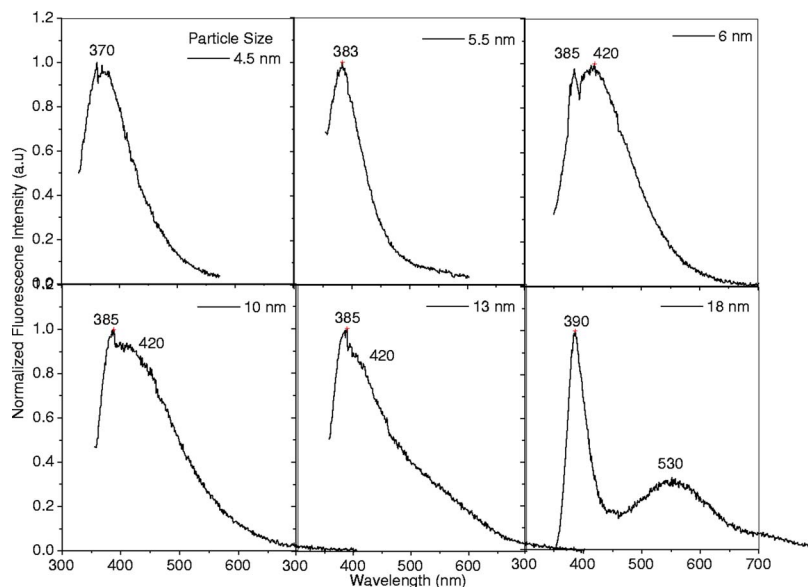


FIG. 8. Fluorescence spectra of nano-ZnO colloids of different particle size for an excitation wavelength of 325 nm.

UV emission with particle size closely follows the redshift in the band edge, indicating that the two are related. This allows us to reconstruct the size distribution curves in the fluorescence spectrum.

In contrast to the UV spectra, visible fluorescence spectra of ZnO particles are sensitive to the preparation procedure (and, therefore, to environmental conditions). The well-known green fluorescence at  $510 \pm 50$  nm appeared in colloids with larger particle size. An additional blue band having peaks at 420 and 490 nm has been observed and in its presence both the UV and 530 nm band is strongly suppressed.

In ZnO, oxygen has tightly bound  $2p$  electrons and Zn tightly bound  $3d$  electrons, which sense the nuclear attraction efficiently. The first principal calculation found that the Zn  $3d$  electrons strongly interact with the O  $2p$  electron in ZnO.<sup>23</sup> As the center energy of the green peak is smaller than the band gap energy of ZnO (3.36 eV), the visible emission cannot be ascribed to the direct recombination of a conduction electron in the Zn  $3d$  band and a hole in the O  $2p$  valence band. The green emission must be related to the local level in band gap. The PL of ZnO has been extensively investigated, and there is no consensus in the literature on the positions of the peaks in PL spectrum of ZnO nanostructures and thin films or their origin.

In nanocolloids of ZnO with large particle size, the surface states are responsible for the green fluorescence. As the particle size increases, the volume fraction of nanoparticles increases due to the specialty of the synthesis route and leads to the dominant role of surface state effects at larger particle size. The polyol synthesis enables one to prepare colloids of different sizes without any surface passivation. Hence, the role of surface states cannot be neglected. Brunauer Emmett and Teller method (BET) surface area measurements are taken using Nova 1200, Quantachrome Instruments and is  $30 \text{ m}^2/\text{g}$  for the powder extracted from colloids of 18 nm. Therefore, the concept of surface fluorescence centers seems to be more realistic for nanoparticles. Researches indicate that the surface passivation via surfactant and polymer cap-

ping is an effective method to enhance the UV emission and quench the defect-related visible PL from nanosized ZnO.<sup>21,24</sup> The effect of method of preparation and surface passivation itself is an indication that the green emission is due to surface states.<sup>12</sup> For the uncapped ZnO nanoparticles, there exist abundant surface defects, the valence band hole can be trapped by the surface defects and then tunnels back into oxygen vacancies containing one electron to form  $V_{\text{O}}^{**}$  recombination center. The recombination of a shallowly trapped electron with a deeply trapped hole in a  $V_{\text{O}}^{**}$  center causes visible emission.<sup>25</sup>

The green emission is commonly referred to a deep-level or a trap-state emission attributed to the singly ionized oxygen vacancy and the emission results from the radiative recombination of photogenerated hole with an electron occupying the oxygen vacancy and Vanheusden *et al.*<sup>9</sup> observed a correlation between the intensities of  $g \sim 1.96$  electron paramagnetic resonance (EPR) peak and green PL. However, the assignment of  $g \sim 1.96$  signal to singly ionized oxygen vacancy is controversial. This signal was also assigned to shallow donors and its position appears to be independent on the shallow donor intensity.<sup>26</sup> Recently, Djuricic *et al.*<sup>12,27</sup> found that there is no simple relationship between the intensity of  $g \sim 1.96$  EPR signal and the visible PL; the green PL is observed for the samples which do not show EPR line at  $g \sim 1.96$ , and they conclude that the most likely explanation for the green luminescence involves multiple defects and/or defect complexes and the major part of the visible emission originates from the centers at the nanostructures surface. Xu *et al.*<sup>28</sup> calculated the levels of various defects including complex defects  $V_{\text{O}}:\text{Zn}_i$  and  $V_{\text{Zn}}:\text{Zn}_i$ . They found no states within the gap from  $V_{\text{Zn}}:\text{Zn}_i$ , whereas for  $V_{\text{O}}:\text{Zn}_i$  two levels 1.2 and 2.4 eV above the valence band were found, so this type of defect represents a possible candidate for green emission in ZnO.

ZnO is an  $n$ -type semiconductor and it means that most defects are Zn interstitials and oxygen vacancies. The crystal structure of ZnO contains large voids which can easily accommodate interstitial atoms<sup>8</sup> and the appearance of blue

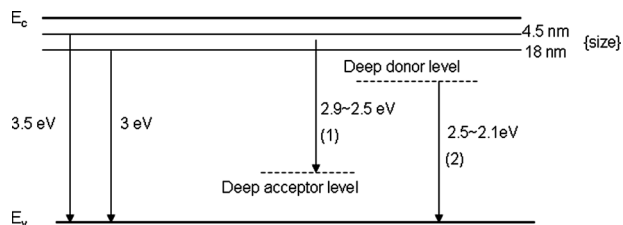


FIG. 9. UV and visible photoluminescence mechanisms of ZnO: (1) transition from near conduction band edge to deep acceptor level and (2) transition from deep donor level to valence band.

emission at about 420 nm is ascribed to the formation of Zn interstitial defects. ZnO nanopowders and thin films also show green luminescence after they were annealed in oxygen, nitrogen or air.<sup>29</sup> The appearance of a strong green emission is ascribed to the formation of oxygen vacancy defects or antisite defects ( $O_{Zn}$ ). There exist many oxygen vacancies on the surface of the ZnO annealed in Ar at 900 °C and shows emission peak at 490 nm while the ZnO annealed in  $O_2$  at 900 °C exhibits emission peak at 530 nm. So the appearance of blue emission at about 490 nm is ascribed to the formation of oxygen vacancy defects, and the emission at 530 nm may have originated the antisite defects ( $O_{Zn}$ ).<sup>29</sup> Thus in our present studies, the appearance of blue emission at about 420 nm is assigned to the Zn interstitial defects, the emission at 490 nm is ascribed to the formation of oxygen vacancy defects and the emission at 530 nm may have originated from the antisite defects ( $O_{Zn}$ ).

Figure 8 shows the fluorescence spectra of nano-ZnO colloids of different particle size for an excitation wavelength of 325 nm. With the decrease of excitation energy, the blue band peaks get suppressed and UV and green fluorescence peak becomes dominant at larger particle size.

Figure 9 shows the emission mechanism of UV and visible luminescence of ZnO colloids. UV luminescence at 3.5 eV is caused by the transition from near conduction band edge to valence band. As particle size increases, the shift of UV luminescence was observed from 3.5 to 3 eV because the optical energy gap decreases from 4 to 3.5 eV. The visible luminescence in the range of 420–530 nm (2.9–2.4 eV) is mainly due to surface state effects. The UV luminescence center is not related to visible luminescence center. Based on these results, the green luminescence of ZnO colloid is not due to the transition from near band edge to deep acceptor level in ZnO but mainly due to the transition from deep donor level by oxygen vacancies in ZnO to valence band. If green luminescence is related to the deep acceptor level, UV luminescence should be decreased as green luminescence increased. As the UV luminescence gets suppressed in the presence of blue band, the blue luminescence is related to the deep acceptor level. These results reveal that the mechanism of blue luminescence in ZnO is by the mechanism which is the transition (1) from near conduction band edge to deep acceptor level and the mechanism of green luminescence is by the mechanism and (2) from deep donor level attributed to the oxygen vacancies to valence band.

#### IV. CONCLUSIONS

In the present work we have performed a size dependent spectroscopic study of the colloidal ZnO particles. In the

fluorescence spectra we have observed two principal bands: (1) UV and (2) visible. The UV band has been assigned to the *band gap* fluorescence of clusters of different sizes. This allows us to reconstruct the size distribution curves from fluorescence spectroscopy. The blue luminescence in ZnO is by the mechanism of the transition from near band edge to deep acceptor level and the green luminescence is by the mechanism of the transition from deep donor level to valence band. The luminescence mechanism can be used to control the optical properties of ZnO for optical device applications.

#### ACKNOWLEDGMENTS

The first author (L.I.) acknowledges UGC for research fellowship. Another author (B.K.) wishes to acknowledge C-MET for the support and permission given to pursue this work.

- <sup>1</sup>Y. Wang and N. Herron, *J. Phys. Chem.* **95**, 525 (1991).
- <sup>2</sup>S. A. Studenikin, M. Cocivera, W. Kellner, and H. Pascher, *J. Lumin.* **91**, 223 (2000).
- <sup>3</sup>S. Nakamura, *The Blue Laser Diode* (Springer, New York, 1997).
- <sup>4</sup>D. C. Reynolds, D. C. Look, and B. Jogai, *Solid State Commun.* **99**, 873 (1996).
- <sup>5</sup>Z. L. Wang, *J. Phys.: Condens. Matter* **16**, R829 (2004).
- <sup>6</sup>L. Brus, *J. Phys. Chem.* **90**, 2555 (1986).
- <sup>7</sup>R. M. Nyffenegger, B. Craft, M. Shaaban, S. Gorer, G. Erley, and R. M. Penner, *Chem. Mater.* **10**, 1120 (1998).
- <sup>8</sup>L. V. Azaroff, *Introduction to Solids* (McGraw-Hill, New York, 1960), pp. 371–372.
- <sup>9</sup>K. Vanheusden, W. L. Warren, C. H. Seager, D. R. Tallant, J. A. Voigt, and B. E. Gnade, *J. Appl. Phys.* **79**, 7983 (1996).
- <sup>10</sup>W. Li, D. Mao, F. Zhang, X. Wang, X. Liu, S. Zou, Y. Zhu, Q. Li, and J. Xu, *Nucl. Instrum. Methods Phys. Res. B* **169**, 59 (2000).
- <sup>11</sup>F. Hache, M. C. Klein, D. Ricard, and C. Flytzanis, *J. Opt. Soc. Am. B* **8**, 1802 (1991).
- <sup>12</sup>D. Li, Y. H. Leung, A. B. Djuricic, Z. T. Liu, M. H. Xie, S. L. Shi, S. J. Xu, and W. K. Chan, *Appl. Phys. Lett.* **85**, 1601 (2004).
- <sup>13</sup>D. Jezequel, J. Guenot, N. Jouini, and F. Fievet, *J. Mater. Res.* **10**, 77 (1995).
- <sup>14</sup>E. W. Seelig, B. Tang, A. Yamilov, H. Cao, and R. P. H. Chang, *Mater. Chem. Phys.* **9712**, 1 (2002).
- <sup>15</sup>R. Viswanatha, Sammer Sapra, B. Satpati, P. V. Satyam, B. N. Dev, D. D. Sharma, *J. Mater. Chem.* **14**, 661 (2004).
- <sup>16</sup>D. Luna-Moreno, E. De la Rosa-Cruz, F. J. Cuevas, L. E. Regalado, P. Salas, R. Rodríguez, and V. M. Castano, *Opt. Mater.* **19**, 275 (2002).
- <sup>17</sup>V. L. Colvin, A. P. Alivisatos, and J. G. Tobin, *Phys. Rev. Lett.* **66**, 2786 (1991).
- <sup>18</sup>S. Sapra and D. D. Sarma, *Phys. Rev. B* **69**, 125304 (2004).
- <sup>19</sup>W. Zhang, H. Wang, K. S. Wong, Z. K. Tang, G. K. L. Wong, and J. Ravinder, *Appl. Phys. Lett.* **75**, 3321 (1999).
- <sup>20</sup>PCPDFWIN v. 2.02 ICDD (JCPDS-International Centre for Diffraction Data, 1999).
- <sup>21</sup>L. Guo, S. Yang, C. Yang, P. Yu, J. Wang, W. Ge, and G. K. L. Wong, *Appl. Phys. Lett.* **76**, 2901 (2000).
- <sup>22</sup>S. W. Kim, S. Fujita, and S. Fujita, *Appl. Phys. Lett.* **81**, 5036 (2002).
- <sup>23</sup>P. Schroer, P. Kruger, and J. Pollmann, *Phys. Rev. B* **47**, 6971 (1993).
- <sup>24</sup>V. A. Fonoberov and A. Balandin, *Appl. Phys. Lett.* **85**, 5971 (2004).
- <sup>25</sup>A. van Dijken, E. A. Meulenkaamp, D. Vanmaekelbergh, and A. Meijerink, *J. Phys. Chem. B* **104**, 1715 (2000).
- <sup>26</sup>N. Y. Garces, N. C. Giles, L. E. Halliburton, G. Cantwell, D. B. Eason, D. C. Reynolds, and L. C. Look, *Appl. Phys. Lett.* **80**, 1334 (2002).
- <sup>27</sup>A. B. Djuricic, W. C. H. Choy, V. A. L. Roy, Y. H. Leung, C. Y. Kwong, K. W. Cheah, T. K. G. Rao, H. F. Lui, and C. Surya, *Adv. Funct. Mater.* **14**, 856 (2004).
- <sup>28</sup>P. S. Xu, Y. M. Sun, C. S. Shi, F. Q. Xu, and H. B. Pan, *Nucl. Instrum. Methods Phys. Res. B* **199**, 286 (2003).
- <sup>29</sup>J. Z. Wang, G. T. Du, Y. T. Zhang, B. J. Zhao, X. T. Yang, and D. L. Liu, *J. Cryst. Growth* **263**, 269 (2004).